

## Research article

# Functional brain changes in auditory phantom perception evoked by different stimulus frequencies

Jeffrey Hullfish<sup>a</sup>, Ian Abenes<sup>a</sup>, Silvia Kovacs<sup>b</sup>, Stefan Sunaert<sup>b</sup>, Dirk De Ridder<sup>c</sup>, Sven Vanneste<sup>a,\*</sup>

<sup>a</sup> School of Behavioral and Brain Sciences, The University of Texas at Dallas, Richardson, TX 75080, USA

<sup>b</sup> Translational MRI, Department of Imaging and Pathology & Medical Imaging Research Center, Department of Radiology, Catholic University of Leuven, Leuven 3000, Belgium

<sup>c</sup> Department of Surgical Sciences, Section of Neurosurgery, Dunedin School of Medicine, University of Otago, Dunedin 9054, New Zealand

## ARTICLE INFO

## Keywords:

Connectivity  
Distress  
fMRI  
Prediction error  
Saliency  
Tinnitus

## ABSTRACT

Bayesian models of brain function such as active inference and predictive coding offer a general theoretical framework with which to explain several aspects of normal and disordered brain function. Of particular interest to the present study is the potential for such models to explain the pathology of auditory phantom perception, i.e. tinnitus. To test this framework empirically, we perform an fMRI experiment on a large clinical sample ( $n = 75$ ) of the human chronic tinnitus population. The experiment features a within-subject design based on two experimental conditions: subjects were presented with sound stimuli matched to their tinnitus frequency (TF) as well as similar stimuli presented at a control frequency (CF). The responses elicited by these stimuli, as measured using both activity and functional connectivity, were then analyzed both within and between conditions. Given the Bayesian-brain framework, we hypothesize that TF stimuli will elicit greater activity and/or functional connectivity in areas related to the cognitive and emotional aspects of tinnitus, i.e. tinnitus-related distress. We conversely hypothesize that CF stimuli will elicit greater activity/connectivity in areas related to auditory perception and attention. We discuss our results in the context of this framework and suggest future directions for empirical testing.

## 1. Introduction

Tinnitus is defined as the perception of sound, typically tones and/or noise, in the absence of a corresponding, external source [1,2]. Since the advent of the neurophysiological model of tinnitus [3], our conception of the disorder has shifted from it being a purely cochlear problem to being a complex pathology of both auditory and non-auditory brain areas and networks [2,4–7]. Phantom perception of sound is often compared to phantom pain [8] and there is a growing body of evidence to suggest that the two disorders are linked [9]. Additionally, an emerging theoretical framework that describes the brain as a prediction machine potentially offers a basis with which to describe not only tinnitus and phantom pain but also several other disorders of phantom perception as maladapted processes of active (Bayesian) inference and predictive coding; see e.g. [4,10,11]. The specific aim of the present study is to test this framework empirically in a clinical sample of the tinnitus population.

We hypothesize that the predictive-brain framework can explain the

pathology of tinnitus [4,10,11], and our model is as follows. First, sensory deafferentation, in this case hearing loss, elicits a prediction error in the auditory system. This prediction error arises because the brain's internal model predicts, but no longer receives, a certain level of auditory input in the deafferented pathway [4]; the prediction in question is a parameter of the prior density over inputs, namely the prior expectation [12]. Because this change in input is statistically reliable—hearing loss is generally permanent, after all—the brain updates its internal model using active (Bayesian) inference to better describe the new distribution of sensory input [13–16]. “Updating” in this case means that the sensitivity of the deafferented cells is increased [17,18], which enables a lower level of neuronal activity to update the model and thus affect perception. However, if these changes are sufficient to allow spontaneous activity in the deafferented cells to update the model, then that noise is treated as signal and thus perceived [11]. In other words, the brain resolves the prediction error resulting from hearing loss but in doing so it learns a causal relationship between spontaneous activity (input) and auditory perception (cause), which

\* Corresponding author at: Lab for Clinical & Integrative Neuroscience, School of Behavioral & Brain Sciences, University of Texas at Dallas, 800 W Campbell Rd, Richardson, Texas 75080, USA.

E-mail address: [sven.vanneste@utdallas.edu](mailto:sven.vanneste@utdallas.edu) (S. Vanneste).

<https://doi.org/10.1016/j.neulet.2018.07.043>

Received 19 April 2018; Received in revised form 24 July 2018; Accepted 30 July 2018

Available online 31 July 2018

0304-3940/ © 2018 Elsevier B.V. All rights reserved.

manifests as a phantom percept. This is an example of maladaptive Bayesian belief updating [10].

Two sounds that differ in frequency but are otherwise identical (e.g. pure tones) should elicit similar neural responses in a healthy brain, barring the difference reflecting the change in frequency itself. However, given our model, we would expect tinnitus-frequency sounds to evoke a different neural response than similar sounds at other frequencies because the maladapted internal model of the tinnitus brain has a prior expectation of the tinnitus percept. In other words, a tinnitus-frequency stimulus should evoke minimal prediction error in perceptual areas—and, in turn, minimal belief updating—because the maladapted model already predicts a similar input. The opposite may be true elsewhere in the brain, such as in areas with a role in the cognitive and emotional components of tinnitus, i.e. tinnitus-related distress.

Previous research suggests that a patient's psychological and emotional state can have a powerful impact on tinnitus perception [19–22]. While sound, unlike pain, is not intrinsically aversive, an estimated 20% of tinnitus patients—1–3% of the general population [2]—report that tinnitus negatively impacts their quality of life. According to the pain literature, modulation of the affect of the pain percept occurs due to a reappraisal of emotional experiences of perception, which is reflected by prefrontal cortex (PFC) communicating with nucleus accumbens (NAc) and the amygdala [23,24]. Increased functional connectivity between NAc and PFC has also predicted the persistence of pain, which implies a causal relationship between corticostriatal circuits and pain chronification [25]. Additional cortical and subcortical regions, including reward/motivation circuits, integrate internal and external signals and encode these signal valuations, while corticolimbic structures engage during the anticipation of the percept [26]. The role of the NAc, mediated by ventral tegmental area (VTA) dopaminergic inputs, appears to be signaling the salience and affective value of incoming stimuli [23,27]. This information is then projected to areas of the frontal lobe such as the ventromedial prefrontal cortex (vmPFC), pregenual anterior cingulate cortex (pgACC), and dorsal anterior cingulate cortex (dACC) that are involved in learning of aversive outcomes and encoding information about the value of a chosen action [28,29]. Tinnitus-related distress appears to be related to functional changes in a disorder-general network involving the amygdala, hippocampus, parahippocampal cortex (PHC), insular cortex, and subgenual ACC (sgACC) [8]. In these areas, we would expect tinnitus-frequency sounds to elicit a greater response than sounds at other frequencies for the simple reason that the latter sounds generally do not have a negative valence. The response in these areas to non-tinnitus sounds should be attenuated either because they mask tinnitus perception and/or because they serve as a distractor, i.e. drawing attention away from the tinnitus percept.

The present study is designed to test our hypotheses directly using an fMRI experiment. We present human chronic tinnitus patients with sounds matched to their tinnitus frequency (TF) and with sounds at a control frequency (CF) while they undergo scanning. We analyze BOLD activity at the whole-brain level as well as in specific regions of interest (ROIs) chosen based on the existing tinnitus literature. Furthermore, we analyze functional connectivity between these ROIs to observe changes at the network level. We hypothesize that TF stimuli will elicit greater activity and functional connectivity specifically in areas related to cognitive and emotional, but not perceptual, aspects of tinnitus. This includes frontostriatal networks [9,25] as well as regions of the general distress network proposed in [8]: amygdala, PHC, insular cortex, and sgACC. Outside of these regions, we hypothesize that CF stimuli will elicit greater activity and functional connectivity.

## 2. Materials and methods

The present study is a retrospective analysis of data collected in a clinical context. Tinnitus patients were recruited at the University Hospital of Antwerp and referred to the Catholic University of Leuven

for MR scanning. All participants provided written informed consent that their data could be used for research purposes per the Declaration of Helsinki. The study was approved by the ethical committee of the University Hospital of Antwerp (IRB: UZA OGA85) and was carried out in accordance with the approved guidelines.

### 2.1. Subjects

The subject group consisted of humans with clinically relevant tinnitus ( $n = 75$ ), defined as being severe enough for the patient to voluntarily seek out treatment [30]. The subjects' ages ranged from 19 to 72 years with a mean age of  $51.0 \pm 11.9$  (SD). 28.0% of subjects were female ( $n = 21$ ). 54.7% of subjects reported that their tinnitus percepts were noise-like ( $n = 41$ ) while 45.3% reported pure-tone percepts ( $n = 34$ ). 46.7% of subjects ( $n = 35$ ) reported unilateral tinnitus, with 28.0% left-lateralized ( $n = 21$ ) and 18.7% right-lateralized ( $n = 14$ ), while 53.3% of subjects reported bilateral or holocranial tinnitus ( $n = 40$ ). Subjects reported tinnitus-related distress using the Tinnitus Questionnaire (TQ), which is scored 0–82 with higher scores corresponding to greater levels of distress [31,32]; the mean TQ score was  $49.3 \pm 16.4$  (SD). All subjects were right-handed.

### 2.2. Audiometry

Before scanning, subjects were screened using pure-tone audiometry to check for hearing loss and to determine any necessary level correction for the experimental stimuli. All patients were screened for the extent of hearing loss, in dB HL, at 0.25, 0.5, 1, 2, 3, 4, 6, and 8 kHz using pure tone audiometry. This was done per the recommended British Society of Audiology procedures, i.e. pure tone air and bone conduction threshold audiometry, with and without masking, plus determination of uncomfortable loudness levels. Fig. 1 shows the mean hearing thresholds for the left and right ears for all tinnitus subjects.

### 2.3. Stimulus frequency selection

A pitch-matching procedure was used to determine behaviorally each subject's tinnitus percept frequency. First, a 1-kHz pure tone was presented contralaterally to the tinnitus ear at a level 10 dB above the patient's hearing threshold in that ear (or the worse ear, in the patients with bilateral or holocranial tinnitus). The frequency of the tone was then adjusted until the patient judged the sound to resemble his/her tinnitus most. This frequency was, on average,  $5.29 \pm 3.38$  (SD) kHz. The stimulus level was adjusted along with frequency to maintain a 10-dB difference above each patient's hearing threshold. Both stimulus level and frequency were checked again within the scanner before starting the experiment.

### 2.4. Experimental procedure

The fMRI experiment consisted of a blocked design of 18 epochs of 30 s each. We presented subjects with three different auditory stimuli binaurally: white noise through a bandpass filter with a 1000-Hz half width ( $f \pm 1000$  Hz); white noise through a bandpass filter with a 500-Hz half width ( $f \pm 500$  Hz); a pure tone ( $f$ ). The center frequencies of the bandpass filters were the same frequency as that of the pure tone. Stimuli were presented in bursts coinciding with the silent gaps between fMRI volume acquisitions, with one stimulus per burst and six epochs per stimulus. Subjects were scanned twice per this design, each at a different frequency,  $f$ . We presented the stimuli to each subject at their tinnitus percept frequency (TF)—chosen via the procedure described in Section 3.3—and at a control frequency (CF) at least one octave higher or lower than the tinnitus frequency; this frequency was, on average,  $1.74 \pm 1.31$  (SD) kHz. The decision to use a higher or lower CF was made on an individual basis such that subjects with a high TF had a low CF and vice versa; only 21.3% of subjects ( $n = 16$ ) had a

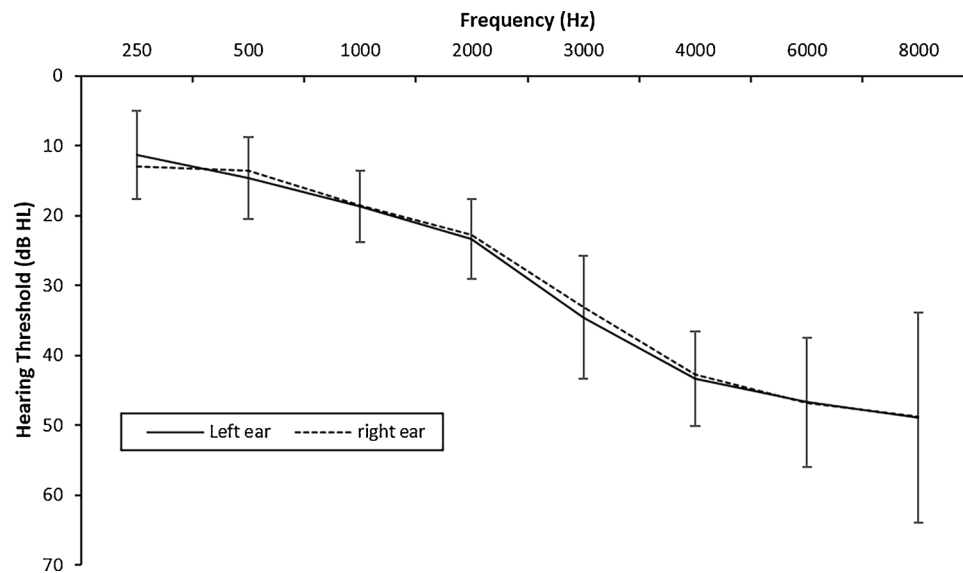


**Fig. 1.** Pure-tone audiograms. Mean pure-tone hearing thresholds in dB HL at frequencies 250–8000 Hz (= .250–8 kHz). The solid line indicates the mean thresholds for the left ears of all subjects ( $n = 75$ ), while the dashed lines indicate the same for the right ears ( $n = 75$ ). Error bars indicate the standard error at each frequency.

CF higher than their TF. The TF/CF presentation order was randomized per subject. Subjects were instructed to listen to the stimuli attentively with their eyes closed. A test run was performed before the start of the experiment to make sure that subjects could hear the stimuli well despite the background scanner noise, which can reach levels of up to 110 dB SPL [33]. All stimuli were presented binaurally through headphones. The headphones were dedicated for use in an MRI scanner, attenuating scanner noise by approximately 30 dB.

## 2.5. Image acquisition and preprocessing

The MRI scans were performed in a Philips 3 T MRI scanner with an eight-channel phased-array head coil. For the functional imaging, a T2\*-weighted single shot gradient echo (GE) echo-planar imaging (EPI) sequence was used with an echo time (TE) and repetition time (TR) of 33 and 5000 ms, respectively (acquisition matrix =  $80 \times 80$ ; field of view =  $230 \times 230 \times 128 \text{ mm}^3$ ; reconstructed voxel size =  $2.88 \times 2.88 \times 4.00 \text{ mm}^3$ ). A clustered volume acquisition technique was used in which the acquisition time (TA) was shorter than the TR, namely 2000 ms, leaving a 3000 ms silent gap in between each EPI volume acquisition. A sensitivity encoding (SENSE) reduction factor of 2.5 was used in the anterior-posterior direction. 32 contiguous, transverse slices of 4 mm thickness each were acquired during 108 dynamics. This resulted in a total scan time of 9 min 30 s per session.

For anatomical reference, an additional high-resolution 3D T1-weighted turbo field echo (TFE) sequence was used with a TE/TR of 4.60/9.60 ms and an acquired voxel size of  $0.98 \times 0.98 \times 1.20 \text{ mm}^3$  (acquisition matrix =  $256 \times 256$ ; field of view =  $250 \times 250 \times 218 \text{ mm}^3$ ; reconstructed voxel size =  $0.98 \times 0.98 \times 1.20 \text{ mm}$ ). SENSE reduction factors of 1.5 and 2 were used in the right-left direction and the anterior-posterior direction, respectively. 182 contiguous, coronal slices were acquired. The resulting total scan time was 6 min 25 s.

Image preprocessing was carried out using SPM12, a third-party software toolbox for Matlab (The MathWorks Inc., Natick, MA) created by the Wellcome Trust Centre for Neuroimaging (<http://www.fil.ion.ucl.ac.uk/spm/software/spm12/>). The anatomical reference image for each subject was skull-stripped and the origin was manually defined at the anterior commissure. The functional image preprocessing pipeline included the following steps: motion correction in six directions; coregistration of functional and structural volumes using a normalized mutual information objective function; normalization of all volumes to MNI standard space; spatial smoothing of functional volumes using an

8-mm full-width at half maximum (FWHM) Gaussian kernel.

## 2.6. Analysis

### 2.6.1. Whole-brain analysis

We analyzed the preprocessed images at the subject level in SPM12. This was done by specifying a general linear model (GLM) design matrix, estimating the parameters for each subject using the restricted maximum likelihood (ReML) method, and generating statistical parametric maps (SPMs). There were ten GLM regressors, including three for the stimuli (WBN, NBN, and PT), six for head motion correction ( $x$ ,  $y$ ,  $z$ , pitch, roll, and yaw), plus a constant. We analyzed the subject-level SPMs at the group level using one-sample  $t$ -tests. We then analyzed the specified designs using ReML to generate a group-level SPM. We checked the  $t$  scores at each voxel in that group-level SPM for significance at the 0.05 level by calculating the corresponding  $p$  values, correcting for multiple comparisons at the voxel level using the false discovery rate (FDR) adjustment [34]. We used *xjview* (<http://www.alivelearn.net/xjview/>) to perform FDR correction and to detect peak regions. We used Python to plot the results using a glass-brain visualizer.

### 2.6.2. ROI analysis

We chose regions of interest (ROIs) based on their relevance to tinnitus and to our model. Given that the present study is focused on tinnitus, i.e. phantom auditory perception, the inclusion of primary auditory cortex (A1) is self-explanatory. In tinnitus, when missing auditory information cannot be retrieved directly from sensory cortex, e.g. in cases of severe hearing loss, PHC is proposed to retrieve the information from memory instead [4]. Posterior cingulate cortex (PCC) is also implicated in tinnitus, especially its connection to the auditory cortex [35]. PCC is also one of the core nodes of the default network and involved with memory, making its potential interactions with PHC interesting in the context of the present study. We also chose a number of ROIs based on their involvement in signaling salience and/or affective value of incoming stimuli. These included: anterior insular cortex (AIC) and dACC, the two core nodes of the salience network [36]; NAc and VTA, two core nodes of the midbrain dopaminergic system; the habenula (Hb), another reward-signaling region [37]; the amygdala, which is most notably involved in signaling negative affect (fear, anxiety, etc.). We did not include a ROI for vmPFC because its boundaries are somewhat ill-defined. Instead, we chose to include both pgACC and

sgACC, which are more clearly defined regions that abut vmPFC and are included in some definitions of vmPFC; see e.g. “vmPFC/scACC” in [9] (subcallosal ACC = subgenual ACC). PgACC is also of specific relevance to our model given its reported involvement in encoding the value of actions [28,29] and in maintaining predictions [38].

We created spherical ROIs ( $n = 19$ ) with a radius of 3 mm, or 1 mm for Hb, using the MarsBaR toolbox [39]. We used term-based meta-analyses via Neurosynth (<http://neurosynth.org>) to search for specific regions and chose our center coordinates based on the voxels that had the highest z-score and then either inverting the x-coordinate to obtain the contralateral ROI or using  $x = 0$  for our midline ROIs (i.e. pgACC, sgACC, and PCC). For example, a search for “auditory cortex” shows a z-score of 21.57 at (-52, -20, 6), i.e. left A1, and so our two A1 ROIs are located at ( $\pm 52$ , -20, 6). The centers of the ROIs for the four smallest anatomical structures—the amygdala, Hb, NAc, and VTA—were identified manually at the subject level using the corresponding anatomical reference images in individual space, i.e. after performing realignment and coregistration but before normalization and smoothing. This was done to preserve the blood oxygen level-dependent (BOLD) signal changes measured in these structures, which are too small to be robust against the normalization and smoothing processes. The coordinates of the centers of all ROIs are presented in Table 1 except for those of the four smallest structures, which are presented separately in Supplementary Table 1.

We obtained ROI-level data by extracting the beta values of the three stimulus regressors in the GLM (i.e. WBN, NBN, and PT) from the voxels of each ROI, which we then averaged across all 108 scans within a session for each subject. We analyzed the group-level distributions of this data in SPSS using a repeated-measures ANOVA, comparing the responses to tinnitus-frequency (TF) and control-frequency (CF) stimulation. All results were checked for significance at the 0.05 level, including the Bonferroni correction for multiple comparisons where  $n = 19$  ROIs.

### 2.6.3. ROI–ROI functional connectivity analysis

We analyzed functional connectivity between ROIs using partial correlations (Matlab `partialcorr()`: <https://www.mathworks.com/help/stats/partialcorr.html>). We calculated these separately for TF and CF, controlling for the effect of tinnitus-related distress (TQ), to analyze the main effect of stimulus frequency. We checked all results for significance at the 0.05 level, including the FDR correction for multiple comparisons, using the method in [40] (Matlab `mafdr()`: <https://www.mathworks.com/help/bioinfo/ref/mafdr.html>). We treated those partial correlations that survived FDR correction as functional connections, which we then visualized as graphs using NeuroMARVL (<http://immersive.erc.monash.edu.au/neuromarvl/>). The exact magnitudes of each surviving connection are presented separately in heat-map form (Matlab `HeatMap()`: <https://www.mathworks.com/help/bioinfo/ref/HeatMap.html>).

**Table 1**  
Region-of-interest coordinates.

Region	Hemisphere	x	y	z
Auditory cortex	Left/Right	$\pm 52$	-20	6
Anterior cingulate cortex	Left/Right	$\pm 6$	24	38
Dorsal ACC	Midline	0	38	4
Pregenuar ACC	Midline	0	26	-10
Subgenual ACC				
Posterior cingulate cortex	Midline	0	53	26
Anterior insula	Left/Right	$\pm 30$	22	-2
Parahippocampal cortex	Left/Right	$\pm 26$	-36	-10

ROIs listed with ‘Left/Right’ hemisphere are two separate regions with the same y and z coordinates. Coordinates for the amygdala, Hb, NAc, and VTA were chosen manually for each subject based on visual inspection of the anatomical reference and are not in MNI space; see Table S1 for these coordinates. There are 19 ROIs in total. All ROIs are 3-mm spheres except for the Hb ROIs, which are 1-mm spheres.

[heatmap.html](#)). Furthermore, we compared partial correlations between conditions by performing Fisher’s Z transformation on the results from each condition, subtracting the Z scores, and then checking the  $\Delta Z$  values for significance at the FDR-corrected 0.05 level [40]. See also Ref [41]. for further analyses based on tinnitus-related distress. As a precautionary measure, we also checked for differences in connectivity according to gender as well as perceived tinnitus location (i.e. unilateral left, right, or bilateral/holocranial) using the same subtraction analysis method; these analyses returned no significant differences in connectivity.

## 3. Results

Whole-brain subtraction analysis showed that, during TF stimulation, subjects had greater BOLD activity in several regions, mainly in frontal cortex, parietal cortex, and the cerebellum in comparison to CF. No regions showed greater BOLD activity during CF. See Fig. 2 for a summary visualization of the results and Table 2 for the specific t scores and p values at the peak voxels of each cluster. In our ROI-level activity analysis, we observed greater activity in response to TF vs. CF stimulation only in left Hb; this result however did not survive Bonferroni correction for multiple comparisons. We did not observe any significant differences in activity in response to CF vs. TF stimulation. See Table 3 for the full results of this analysis.

Analyses of ROI–ROI functional connectivity produced several results. While both TF and CF stimuli elicited strong functional connectivity between several of our ROIs, CF elicited more connectivity by far in terms of degree (Figs. 3, 4). Subtraction analysis shows that nearly all of the tested connections are significantly different between the two conditions even after correcting for multiple comparisons (Fig. 5). Furthermore, the majority of these differences indicate that CF elicits greater functional connectivity between our ROIs. We do observe greater TF connectivity between right A1 and left dACC, left Hb, right NAc, PCC, and sgACC. There are also several regions where the differences are lateralized. We see this, for example, in connections with bilateral AIC, which has stronger connections to dACC and Hb in the left hemisphere during CF and in the right hemisphere during TF. There are also several lateralized differences in the amygdalar connectivity, including with NAc, PCC, pgACC, and VTA. Furthermore, right VTA has stronger TF connectivity with dACC, Hb, and left NAc. Bilateral VTA features stronger TF connectivity for several regions, as well, including left amygdala, right NAc, and bilateral PHC. However, to reiterate, the majority of the observed differences in connectivity are greater during CF than TF stimulation.

## 4. Discussion

The aim of the present study was to examine changes in the brains of chronic tinnitus patients in response to tinnitus-frequency (TF) and control-frequency (CF) sound stimuli, as measured using fMRI. Under the predictive-brain framework, we hypothesized that TF stimuli would evoke less activity/connectivity in areas related to auditory perception and more activity/connectivity in areas related to the cognitive and emotional aspects of tinnitus, e.g. tinnitus-related distress. We hypothesized the opposite pattern in response to CF stimuli. Our results are consistent with these hypotheses in some instances and less so in others. We discuss those results in more depth here in an effort to refine our hypotheses and to suggest how future studies might improve upon the present design to explore these ideas further.

Looking first at the whole-brain analyses, subtraction of the responses during TF and CF stimulation reveals several areas with increased activity. During TF stimulation, subjects exhibit greater activity in the lateral surfaces of frontal cortex—especially in the middle and inferior frontal gyri of the left hemisphere—and the cerebellum as well as in the right orbitofrontal, right parietal, and left middle temporal cortices. Many of these TF-activated regions resemble an extended

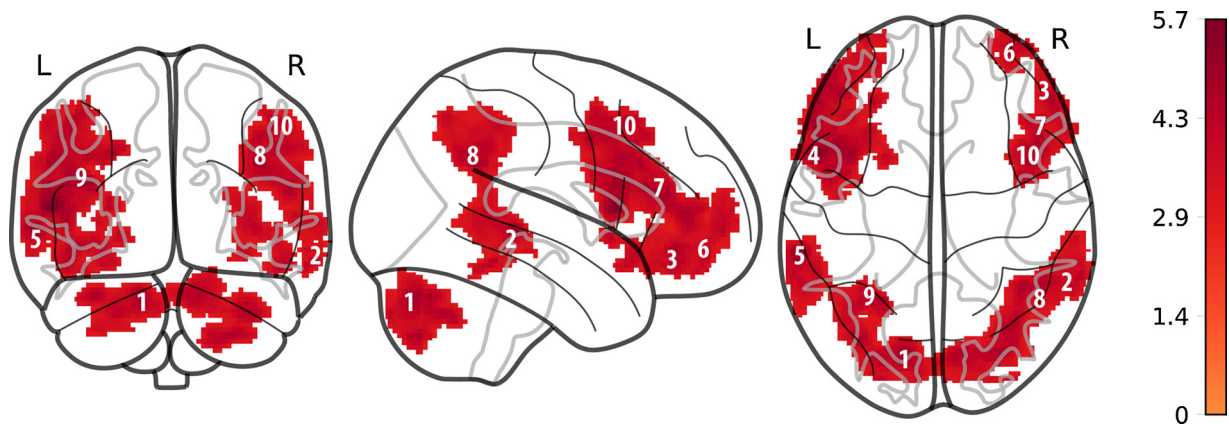


**Fig. 2.** Whole-brain subtraction analysis, TF vs. CF. Glass brain view of a subtraction analysis comparing the TF and CF experimental conditions for all subjects ( $n = 75$ ;  $df = 74$ ). Colored voxels indicate where TF > CF; analysis revealed no statistically significant clusters where CF > TF. The height threshold is set at FDR-corrected  $p < 0.05$  ( $\approx$  uncorrected  $p < 1.60 \times 10^{-3}$ ); the cluster size threshold is set at 200 voxels. The numbers overlaid on the voxels approximately indicate the locations of the peak regions of the clusters listed in Table 2.

**Table 2**  
Whole-brain analysis, TF vs. CF.

Cluster	Peak region	Hemisphere	x	y	z	Size	t	p
1	Cerebellum, Crus	Left	-14	-80	-30	1909	4.89	$2.87 \times 10^{-6}$
2	Middle Temporal Gyrus	Right	66	-42	-14	331	4.49	$1.29 \times 10^{-5}$
3	Orbitofrontal Cortex	Right	52	38	-16	211	4.45	$1.50 \times 10^{-5}$
4	Frontal Inferior Operculum	Left	-54	12	10	3412	5.72	$1.07 \times 10^{-7}$
5	Middle Temporal Gyrus	Left	-62	-32	0	683	5.16	$1.02 \times 10^{-6}$
6	Middle Frontal Gyrus	Right	38	62	0	263	4.28	$2.76 \times 10^{-5}$
7	Inferior Frontal Gyrus, Pars Triangularis	Right	54	36	18	767	4.74	$5.06 \times 10^{-6}$
8	Supramarginal Gyrus	Right	38	-52	30	691	4.80	$4.10 \times 10^{-6}$
9	Angular Gyrus	Left	-26	-54	34	488	4.67	$6.69 \times 10^{-6}$
10	Middle Frontal Gyrus	Right	46	18	50	290	4.71	$5.73 \times 10^{-6}$

Clusters and peak region names were determined automatically in xjview using the Automated Anatomical Labeling (AAL) atlas. Coordinates shown are those of the peak voxels for each cluster. Positive  $t$  scores indicate clusters where TF > CF; negative  $t$  scores indicate clusters where CF > TF (note: no clusters were observed where CF > TF). The cluster size threshold is set at 200 voxels; the listed  $p$  values are uncorrected but they are thresholded at  $p < 1.60 \times 10^{-3}$  (i.e. FDR-corrected  $p < 0.05$ );  $df = 74$ .

**Table 3**  
Region of interest analysis, TF vs. CF.

ROI	Hemisphere	F	p
A1	Left	.08	0.77
	Right	.16	0.65
amygdala	Left	1.60	0.21
	Right	.01	0.93
AIC	Left	.06	0.81
	Right	.10	0.75
dACC	Left	.04	0.85
	Right	.07	0.79
Hb	Left	4.97	0.03*
	Right	.002	0.96
NAc	Left	.43	0.51
	Right	.37	0.55
PHC	Left	.77	0.38
	Right	.51	0.48
PCC	Midline	.02	0.88
pgACC	Midline	.07	0.79
sgACC	Midline	.12	0.73
VTA	Left	.21	0.65
	Right	1.00	0.32

Analyses include distress data (TQ scores) as a covariate. Asterisks indicate  $p < 0.05$  (uncorrected); no results survived Bonferroni correction for multiple comparisons calculated using  $n = 19$  ROIs.

cortical network for semantic cognition, which involves the representation and control of semantic knowledge [42]. This is of interest to the present study because semantic knowledge includes the meaning

of sounds. While TF stimuli are less novel to tinnitus patients than CF stimuli, at least hypothetically, they should also have more meaning, given their similarity to the tinnitus percept and the presence of tinnitus-related distress. Outside of this network, orbitofrontal cortex plays a documented role in emotion as well as cognition. Taken together, our results appear to indicate that TF stimuli do elicit greater activity in areas relating to cognitive and emotional aspects of tinnitus.

With that said, the regions observed in our activity analyses do not include the regions that we had specifically hypothesized. Furthermore, none of the voxels that exhibited greater activity during CF survived correction for multiple comparisons. This is reflected in our ROI-level activity analysis, which returned no positive results for TF or CF after correction for multiple comparisons. Therefore, our activity analyses ultimately produced mixed results. One possible explanation is that the TF and CF stimuli, which were identical except for their frequencies, were too similar to elicit differences of the magnitude that we had expected. If the differences are present and merely small in terms of effect size, a larger number of subjects would raise statistical power and potentially allow more of those voxels to survive correction for multiple comparisons. We might also increase the effect sizes themselves by more closely matching the TF stimuli to the tinnitus percept and/or by making the difference between TF and CF stimuli more pronounced yet still similar enough to serve as a within-subject control, as in the present study. Incorporating any—or ideally all—of these approaches would likely produce more definitive results.

Our analyses of ROI–ROI functional connectivity produced several results, many of which were unexpected. The most striking difference

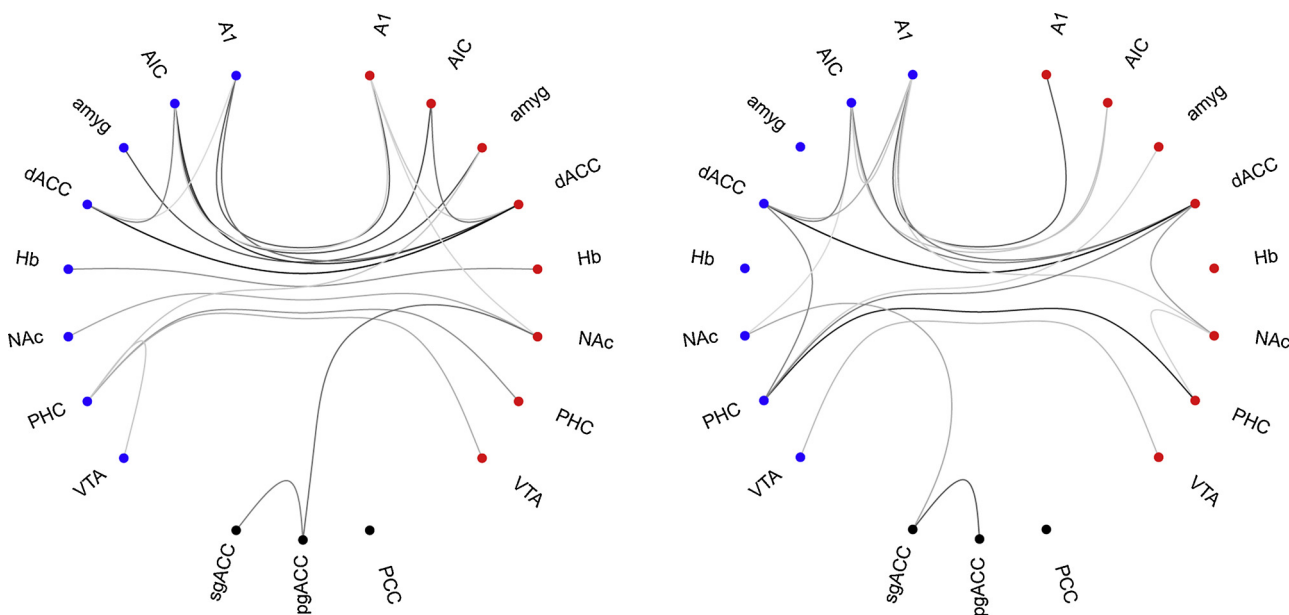


**Fig. 3.** Graph visualization of functional connectivity, TF vs. cf. The left graph shows the functional connectivity for all subjects ( $n = 75$ ) during TF while the right graph shows the same during CF. Functional connectivity is calculated using partial correlation, including tinnitus-related distress (TQ score) as a covariate. The nodes are colored and grouped according to their respective locations, i.e. ROIs in the left and right hemispheres are shown as blue and red nodes, respectively, while ROIs at the midline are shown as black nodes. Edges represent functional connections (i.e. partial correlations) and are colored from gray to black to capture the relative magnitude of each connection within each subfigure, with black encoding the maximum value; the exact values for connection strengths are presented separately in Fig. 4. All displayed edges represent partial correlations that are significant at the 0.05 level, including the FDR correction for multiple comparisons. (For interpretation of the references to colour in this figure legend, the reader is referred to the web version of this article.)

between the TF and CF conditions is that CF stimulation elicits a much higher degree of connectivity between our ROIs. This is evident even when looking at the results within each condition but especially when looking at the subtraction analysis between conditions. There are two possible explanations for this, the first of which comes from our activity analyses: our a priori choice of ROIs did not overlap with the areas which featured greater activity during TF vs. CF stimulation. Secondly,

if the TF-related increases in connectivity are due to tinnitus-related distress, then our choice of TQ score as a covariate would have blunted those effects. We used TQ score as a covariate to mitigate the potentially confounding influence of tinnitus-related distress on our analyses, but this necessarily limits our ability to observe distress-related differences. On one hand, to the extent that this choice means that the observed differences are purely the result of perceptual prediction errors,

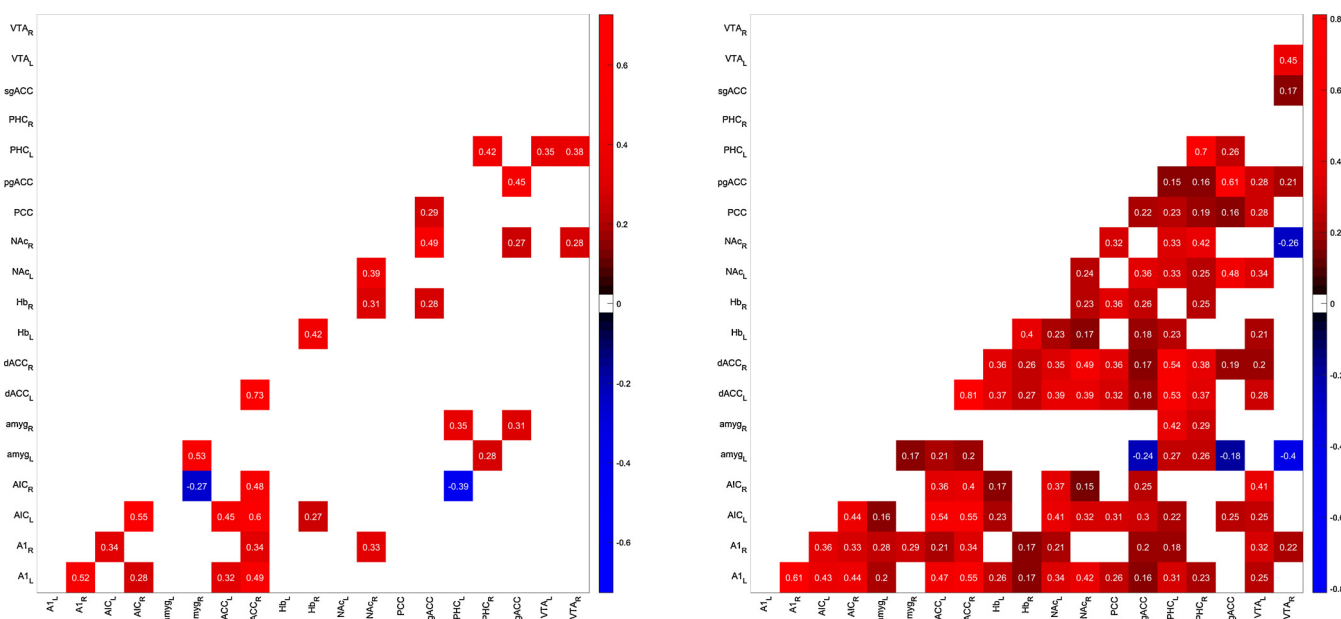


**Fig. 4.** Heatmap visualization of functional connectivity, TF vs. cf. The left heatmap shows the functional connectivity for all subjects ( $n = 75$ ) during TF while the right heatmap shows the same during CF. Functional connectivity is represented here as partial correlations, including tinnitus-related distress (TQ score) as a covariate. The ROIs are labeled along the axes and each colored cell represents a functional connection between two ROIs that is statistically significant at the 0.05 level, including the FDR correction for multiple comparisons. Red and blue cells indicate positive and negative partial correlations, respectively, and the exact value of each connection is presented within each cell. (For interpretation of the references to colour in this figure legend, the reader is referred to the web version of this article.)



## References

- [1] J.J. Eggermont, L.E. Roberts, The neuroscience of tinnitus, *Trends Neurosci.* 27 (2004) 676–682, <https://doi.org/10.1016/j.tins.2004.08.010>.
- [2] A.B. Elgoyhen, B. Langguth, D. De Ridder, S. Vanneste, Tinnitus: perspectives from human neuroimaging, *Nat. Rev. Neurosci.* 16 (2015) 632–642, <https://doi.org/10.1038/nrn4003>.
- [3] J.W. Hazell, P.J. Jastreboff, Tinnitus I: auditory mechanisms: a model for tinnitus and hearing impairment, *J. Otolaryngol.* 19 (1990) 1–5 (accessed July 12, 2016), <http://www.ncbi.nlm.nih.gov/pubmed/2179573>.
- [4] D. De Ridder, S. Vanneste, W. Freeman, The Bayesian brain: phantom percepts resolve sensory uncertainty, *Neurosci. Biobehav. Rev.* 44 (2014) 4–15, <https://doi.org/10.1016/j.neubiorev.2012.04.001>.
- [5] D. De Ridder, S. Vanneste, N. Weisz, A. Londero, W. Schlee, A.B. Elgoyhen, B. Langguth, An integrative model of auditory phantom perception: tinnitus as a unified percept of interacting separable subnetworks, *Neurosci. Biobehav. Rev.* 44 (2014) 16–32, <https://doi.org/10.1016/j.neubiorev.2013.03.021>.
- [6] A.M. Leaver, A. Seydell-Greenwald, T.K. Turesky, S. Morgan, H.J. Kim, J.P. Rauschecker, Cortico-limbic morphology separates tinnitus from tinnitus distress, *Front. Syst. Neurosci.* 6 (2012) 21, <https://doi.org/10.3389/fnsys.2012.00021>.
- [7] A.M. Leaver, T.K. Turesky, A. Seydell-Greenwald, S. Morgan, H.J. Kim, J.P. Rauschecker, Intrinsic network activity in tinnitus investigated using functional MRI, *Hum. Brain Mapp.* 37 (2016) 2717–2735, <https://doi.org/10.1002/hbm.23204>.
- [8] D. De Ridder, A.B. Elgoyhen, R. Romo, B. Langguth, Phantom percepts: tinnitus and pain as persisting aversive memory networks, *Proc. Natl. Acad. Sci. U. S. A.* 108 (2011) 8075–8080, <https://doi.org/10.1073/pnas.1018466108>.
- [9] J.P. Rauschecker, E.S. May, A. Maudoux, M. Ploner, Frontostriatal gating of tinnitus and chronic pain, *Trends Cogn. Sci.* 19 (2015) 567–578, <https://doi.org/10.1016/j.tics.2015.08.002>.
- [10] A. Mohan, S. Vanneste, Adaptive and maladaptive neural compensatory consequences of sensory deprivation—from a phantom percept perspective, *Prog. Neurobiol.* 153 (2017) 1–17, <https://doi.org/10.1016/j.pneurobio.2017.03.010>.
- [11] W. Sedley, K.J. Friston, P.E. Gander, S. Kumar, T.D. Griffiths, An integrative tinnitus model based on sensory precision, *Trends Neurosci.* 39 (2016) 799–812, <https://doi.org/10.1016/j.tins.2016.10.004>.
- [12] K. Friston, Learning and inference in the brain, *Neural Netw.* 16 (2003) 1325–1352, <https://doi.org/10.1016/j.neunet.2003.06.005>.
- [13] K. Friston, A theory of cortical responses, *Philos. Trans. R. Soc. Lond. B. Biol. Sci.* 360 (2005) 815–836, <https://doi.org/10.1098/rstb.2005.1622>.
- [14] K. Friston, J. Kilner, L. Harrison, A free energy principle for the brain, *J. Physiol. Paris* 100 (2006) 70–87, <https://doi.org/10.1016/j.jphysparis.2006.10.001>.
- [15] K. Friston, The free-energy principle: a unified brain theory? *Nat. Rev. Neurosci.* 11 (2010) 127–138, <https://doi.org/10.1038/nrn2787>.
- [16] K. Friston, C. Thornton, A. Clark, Free-energy minimization and the dark-room problem, *Front. Psychol.* 3 (2012) 1–7, <https://doi.org/10.3389/fpsyg.2012.00130>.
- [17] P. Sterling, S. Laughlin, Principles of Neural Design, MIT Press, 2015, <https://doi.org/10.1017/CBO9781107415324.004>.
- [18] P. Sterling, Principles of allostasis: optimal design, predictive regulation, pathophysiology, and rational therapeutics, in: J. Schulkin (Ed.), Allostasis, Homeostasis, Costs Physiol. Adapt. Cambridge University Press, 2004, pp. 17–64, <https://doi.org/10.1017/CBO9781316257081.004>.
- [19] M.C. Bushnell, M. Čeko, L.A. Low, Cognitive and emotional control of pain and its disruption in chronic pain, *Nat. Rev. Neurosci.* 14 (2013) 502–511, <https://doi.org/10.1038/nrn3516>.
- [20] T. Probst, R. Pryss, B. Langguth, W. Schlee, Emotion dynamics and tinnitus: daily life data from the “TrackYourTinnitus” application, *Sci. Rep.* 6 (2016) 31166, <https://doi.org/10.1038/srep31166>.
- [21] T. Probst, R. Pryss, B. Langguth, W. Schlee, Emotional states as mediators between tinnitus loudness and tinnitus distress in daily life: results from the “TrackYourTinnitus” application, *Sci. Rep.* 6 (2016) 1–8, <https://doi.org/10.1038/srep20382>.
- [22] K. Wiech, I. Tracey, The influence of negative emotions on pain: behavioral effects and neural mechanisms, *Neuroimage.* 47 (2009) 987–994, <https://doi.org/10.1016/j.neuroimage.2009.05.059>.
- [23] E. Navratilova, F. Porreca, Reward and motivation in pain and pain relief, *Nat. Rev. Neurosci.* 17 (2014) 1304–1312, <https://doi.org/10.1038/nrn3811>.
- [24] T.D. Wager, M.L. Davidson, B.L. Hughes, M.A. Lindquist, K.N. Ochsner, Prefrontal-subcortical pathways mediating successful emotion regulation, *Neuron.* 59 (2008) 1037–1050, <https://doi.org/10.1016/j.neuron.2008.09.006>.
- [25] M.N. Baliki, B. Petre, S. Torbey, K.M. Herrmann, L. Huang, T.J. Schnitzer, H.L. Fields, A.V. Apkarian, Corticostriatal functional connectivity predicts transition to chronic back pain, *Nat. Neurosci.* 15 (2012) 1117–1119, <https://doi.org/10.1038/nn.3153>.
- [26] T.D. Wager, Placebo-induced changes in fMRI in the anticipation and experience of pain, *Science.* 54 (2004) 155–161, <https://doi.org/10.1126/science.1093065>.
- [27] W. Schultz, Updating dopamine reward signals, *Curr. Opin. Neurobiol.* 23 (2013) 229–238, <https://doi.org/10.1016/j.conb.2012.11.012>.
- [28] M.P. Noonan, M.E. Walton, T.E.J. Behrens, J. Sallet, M.J. Buckley, M.F.S. Rushworth, Separate value comparison and learning mechanisms in macaque medial and lateral orbitofrontal cortex, *Proc. Natl. Acad. Sci.* 107 (2010) 20547–20552, <https://doi.org/10.1073/pnas.1012246107>.
- [29] M.F.S. Rushworth, M.P. Noonan, E.D. Boorman, M.E. Walton, T.E. Behrens, Frontal Cortex and Reward-Guided Learning and Decision-Making, *Neuron.* 70 (2011) 1054–1069, <https://doi.org/10.1016/j.neuron.2011.05.014>.
- [30] D. McFadden, Tinnitus: Facts, Theories, and Treatments, Washington, D.C. (1982) <https://books.google.com/books?id=bEYrAAAAyAAJ>.
- [31] R.S. Hallam, S.C. Jakes, R. Hinchcliffe, Cognitive variables in tinnitus annoyance, *Br. J. Clin. Psychol.* 27 (Pt 3) (1988) 213–222, <https://doi.org/10.1111/j.2044-8260.1988.tb00778.x>.
- [32] S. Vanneste, M. Plazier, E. van der Loo, P. Van de Heyning, M. Congedo, D. De Ridder, The neural correlates of tinnitus-related distress, *Neuroimage* 52 (2010) 470–480, <https://doi.org/10.1016/j.neuroimage.2010.04.029>.
- [33] M. Smits, S. Kovacs, D. de Ridder, R.R. Peeters, P. van Hecke, S. Sunaert, Lateralization of functional magnetic resonance imaging (fMRI) activation in the auditory pathway of patients with lateralized tinnitus, *Neuroradiology* 49 (2007) 669–679, <https://doi.org/10.1007/s00234-007-0231-3>.
- [34] Y. Hochberg, Y. Benjamini, Controlling the false discovery rate: a practical and powerful approach to multiple testing, *J. R. Stat. Soc.* 57 (1995) 289–300 <http://www.jstor.org/stable/2346101>.
- [35] A.N. Silchenko, I. Adamchik, C. Hauptmann, P.A. Tass, Impact of acoustic co-ordinated reset neuromodulation on effective connectivity in a neural network of phantom sound, *Neuroimage* 77 (2013) 133–147, <https://doi.org/10.1016/j.neuroimage.2013.03.013>.
- [36] W.W. Seeley, V. Menon, A.F. Schatzberg, J. Keller, G.H. Glover, H. Kenna, A.L. Reiss, M.D. Greicius, Dissociable intrinsic connectivity networks for salience processing and executive control, *J. Neurosci.* 27 (2007) 2349–2356, <https://doi.org/10.1523/JNEUROSCI.5587-06.2007>.
- [37] S. Russo, E. Nestler, The brain reward circuitry in mood disorders, *Nat. Rev. Neurosci.* 625 (2013) 609–625, <https://doi.org/10.1038/nrn3381>.
- [38] D. De Ridder, S. Vanneste, G. Gillett, P. Manning, P. Glue, B. Langguth, Psychosurgery reduces uncertainty and increases free will? A review, *Neuroimaging.* 19 (2016) 239–248, <https://doi.org/10.1111/ner.12405>.
- [39] M. Brett, J.L. Anton, R. Valabregue, J.B. Poline, Region of interest analysis using an SPM toolbox, *Neuroimage.* 16 (2002) 497, [https://doi.org/10.1016/S1053-8119\(02\)90010-8](https://doi.org/10.1016/S1053-8119(02)90010-8).
- [40] J.D. Storey, A direct approach to false discovery rates, *J. R. Stat. Soc. Ser. B* 64 (2002) 479–498.
- [41] J.A. Hullfish, I. Abenes, S. Kovacs, S. Sunaert, D. De Ridder, S. Vanneste, Functional connectivity analysis of fMRI data collected from human subjects with chronic tinnitus and varying levels of tinnitus-related distress (submitted), *Data Br.* (2018).
- [42] C. Whitney, M. Kirk, J. O’Sullivan, M.A. Lambon Ralph, E. Jefferies, The neural organization of semantic control: TMS evidence for a distributed network in left inferior frontal and posterior middle temporal gyrus, *Cereb. Cortex* 21 (2011) 1066–1075, <https://doi.org/10.1093/cercor/bhq180>.